

Vector leptoquark contributions to lepton dipole moments

Arvind Bhaskar,^{1,*} Diganta Das,^{2,†} Soumyadip Kundu,^{3,‡} Anirudhan A. Madathil,^{4,§} Tanumoy Mandal,^{3,¶} and Subhadip Mitra^{2,5,**}

¹*Institute of Physics, Sachivalaya Marg, Bhubaneswar 751 005, India*

²*Center for Computational Natural Sciences and Bioinformatics,*

International Institute of Information Technology, Hyderabad 500 032, India

³*Indian Institute of Science Education and Research Thiruvananthapuram, Vithura, Kerala, 695 551, India*

⁴*Department of Physics and Astronomy, University of Utah, Salt Lake City, UT 84112, USA*

⁵*Center for Quantum Science and Technology, International Institute of Information Technology, Hyderabad 500 032, India*

Leptoquarks (LQs) can contribute to the magnetic and electric dipole moments of charged leptons, which the current experiments have measured with good accuracy. We revisit the parameter spaces of TeV-scale vector LQs that contribute to these observables and study how these models fare against the LHC bounds. We show that significant portions of the parameter space are excluded when the current LHC data is utilised effectively. We find that only U_1 and V_2 can explain the observed positive shift in $(a_\mu^{\text{exp}} - a_\mu^{\text{SM}})$ through a lepton chirality-flipping contribution with $\mathcal{O}(1)$ LQ-quark-lepton coupling. We also see how these two LQs can fit the electron dipole moment and atomic parity violation measurements. We find that the current electric dipole moment measurements of the muon cannot restrain the LQ-quark-lepton couplings within perturbative regions.

I. INTRODUCTION

The Standard Model (SM) predictions for the lepton anomalous magnetic dipole moments [AMDMs, $(g-2)_\ell$] are precise, and the light-lepton ones are also measured experimentally with remarkable accuracy (see, e.g., [1]). Therefore, even a minor discrepancy between the theoretical and experimental values poses severe challenges to the two sides. Robust and consistent experimental measurements prompt a revisit to the theoretical computations, which are highly complex. Conversely, a strong confidence in our SM calculations demands a re-evaluation of the experiments and more precise measurements. A disagreement between theoretical and experimental values of $(g-2)_\mu$ has remained unresolved for more than two decades: the SM expectation for the muon AMDM is $a_\mu^{\text{SM}} = (g-2)_\mu^{\text{SM}}/2 = 116591810(43) \times 10^{-11}$ [2, 3], whereas the current experimental world average reported by the Muon $g-2$ Collaboration is $a_\mu^{\text{exp}} = 116592059(22) \times 10^{-11}$ [1, 4]. The experimental value is about 5σ away from the SM expectation, i.e., $\Delta a_\mu = a_\mu^{\text{exp}} - a_\mu^{\text{SM}} = (2.49 \pm 0.48) \times 10^{-9}$. If we trust both the SM predictions and experimental measurements, we can take this discrepancy as a hint of the presence of new physics (NP) beyond the SM.

The $(g-2)_\mu$ anomaly has several possible NP explanations (see Ref. [5] for a recent review and the references). Prominent among these are the models featuring leptoquarks (LQs or ℓ_q)—hypothetical bosons that couple simultaneously to a lepton and a quark. The lepton and quark sectors in the SM are similar—both have three generations—and this parity is necessary to cancel the gauge anomalies. However, these similarities perhaps also

suggest a deeper connection between these two sectors. Within the unified theory framework, leptons and quarks naturally couple through LQs [6, 7]. In various theories with extended gauge symmetries, vector LQs (vLQs) arise when the symmetries break spontaneously. Though less explored than their scalar counterparts (e.g., Ref. [8]), vLQ models have been considered as possible solutions to the $(g-2)_\mu$ anomaly [9, 10]. The difficulty in obtaining consistent ultraviolet-complete theories with vLQs has been the main obstacle in this direction. However, some such solutions are known, e.g., the 4321 model [11]. In such a framework, one can consistently calculate higher-loop effects involving vLQs. These effects in various vLQ models have been discussed in Ref. [12]. TeV-scale vLQs that appear in different phenomenological variants of the Pati-Salam model [11, 13–15] or the composite GUT framework [16] can explain various flavour anomalies. In some bottom-up studies, vLQ models with various flavour ansatzes for the new couplings (i.e., vLQ-quark-lepton couplings) have been used to address multiple anomalies simultaneously [17–19].

The current LHC data strongly constrains the parameter spaces of TeV-scale LQ models. The nonresonant LQ production (i.e., t -channel LQ exchanges) and its interference with the SM can significantly contribute to the invariant-mass distribution of high- p_T lepton pairs. (This distribution is also influenced by additional contributions from resonant pair and single LQ productions, particularly in the low-mass region. Combining both resonant and nonresonant (including interference) contributions and utilising the high- p_T dilepton search data, Refs. [20–22] showed the LQ parameter space to be highly constrained in general.) The bounds from high- p_T di-muon and di-tau data on vLQ couplings can be seen from Ref. [21] and Refs. [15, 18, 19], respectively. Recasting the direct LQ search data in the dilepton-dijet channels [22, 23] also gives strong constraints. The LHC phenomenologies of various LQs have been well-explored—they show good prospects at the LHC (see, e.g., Refs. [24]).

Unlike the scalar LQs, a summary of the status of vLQ

* arvind.bhaskar@iopb.res.in

† diganta.das@iiit.ac.in

‡ soumyadip23@iisertvm.ac.in

§ anirudhan.alanthatta@utah.edu

¶ tanumoy@iisertvm.ac.in

** subhadip.mitra@iiit.ac.in

source of CP violation. A vLQ with a tree-level coupling to the muon and a quark contributes to $(g-2)_\mu$ at the one-loop level; Fig. 1 shows the representative Feynman diagrams. LQs without a tree-level $q\mu\ell_q$ coupling can still contribute to $(g-2)_\mu$ at higher-loop levels. In that case, however, the coupling(s) relevant to the $(g-2)_\mu$ anomaly must be large enough to compensate for the extra loop suppression. Here, we only focus on those vLQs that contribute to $(g-2)_\ell$ at the one-loop level.

In principle, vLQs can have additional diquark interactions leading to proton instability. However, it is possible to construct ultraviolet-complete models with TeV-scale vLQs evading proton lifetime bounds [13]. In such models, the baryon number-violating operators are suppressed or forbidden by some discrete symmetry. For phenomenological purposes, we ignore the diquark couplings. We also neglect the possibility of vLQs interacting with another new particle. We consider up-aligned and down-aligned scenarios (where the vLQ mass basis aligns with the mass basis of the up-type or down-type quarks, respectively) for the vLQs coupling to the left-handed quarks separately. There is only one scenario for the vLQs coupling exclusively to right-handed quarks.

A. Weak-singlet vector leptoquarks

There are two weak-singlet vLQs— $U_1(\mathbf{3}, \mathbf{1}, 2/3)$ and $\tilde{U}_1(\mathbf{3}, \mathbf{1}, 5/3)$ —which can contribute to $(g-2)_\ell$ in principle. Their gauge interactions and mass terms can be generically written as

$$\mathcal{L} \supset -\frac{1}{2}V_{\mu\nu}^\dagger V^{\mu\nu} + ig_s V_\mu^\dagger T_a V_\nu \left(\kappa_s G_a^{\mu\nu} + \tilde{\kappa}_s \tilde{G}_a^{\mu\nu} \right) + ig' Y V_\mu^\dagger V_\nu \left(\kappa_Y B^{\mu\nu} + \tilde{\kappa}_Y \tilde{B}^{\mu\nu} \right) + M_V^2 V_\mu^\dagger V^\mu, \quad (2)$$

where $V^{\mu\nu} = D^\mu V^\nu - D^\nu V^\mu$ is the field-strength tensor of the vLQ V^μ . Here, $G_a^{\mu\nu}$ and $B^{\mu\nu}$ are the SM gauge field-strength tensors and $\tilde{G}_a^{\mu\nu} = \frac{1}{2}\epsilon^{\mu\nu\rho\sigma}G_{\rho\sigma}^a$ and $\tilde{B}^{\mu\nu} = \frac{1}{2}\epsilon^{\mu\nu\rho\sigma}B_{\rho\sigma}$ are the corresponding dual tensors. The anomalous couplings of vLQs are denoted by κ [42]. After the electroweak-symmetry breaking, the electromagnetic interactions of V^μ can be written as

$$\mathcal{L} \supset ieQ \left\{ (\partial^\mu V^\nu - \partial^\nu V^\mu) A_\mu V_\nu^\dagger - (\partial_\mu V_\nu^\dagger - \partial_\nu V_\mu^\dagger) A^\mu V^\nu - \kappa_Y (V_\mu V_\nu^\dagger - V_\nu V_\mu^\dagger) \partial^\mu A^\nu - \frac{1}{2} \tilde{\kappa}_Y \epsilon^{\mu\nu\rho\sigma} (V_\rho V_\sigma^\dagger - V_\sigma V_\rho^\dagger) \partial_\mu A_\nu \right\}. \quad (3)$$

The interactions of U_1 and \tilde{U}_1 with the SM quarks and leptons are shown in Table I. With appropriate flavour ansatzes, the singlet vLQs can produce the required positive shift to a_μ from the SM value to the experimental value. Their contributions to a_μ can be obtained from the general expression shown in Appendix A. These expressions agree with the ones given in Ref. [10].¹ From

Eq. (A2), we see that for free x_1^{XX} couplings, a_ℓ has a logarithmic dependence on the UV-cutoff scale Λ unless $\kappa_Y = 1$ and $\tilde{\kappa}_Y = 0$. [The appearance of the divergent terms is the consequence of adding a gauge boson by hand without considering the full gauge structure. In UV complete theories, κ_Y and $\tilde{\kappa}_Y$ can take different values since the divergences are cancelled by the presence of some other field(s).] The divergent terms vanish for $\kappa_Y = 1$ and $\tilde{\kappa}_Y = 0$. Hence, we retain this choice throughout the paper to avoid divergences in our calculations.

There are two types of contribution to a_μ from a U_1 —a chirality-flipping part that goes as $x_1^{LL} x_1^{RR}$ and is proportional to $m_\mu m_q$ (where q is the quark that runs in the loops; for U_1 it is a down type quark) and a chirality-preserving part proportional to $(|x_1^{LL}|^2 + |x_1^{RR}|^2)$ and m_μ^2 . When q is a bottom quark, the chirality-flipping contribution is more significant for couplings of similar magnitudes. If the quark in the loop is a strange quark, both the chirality-flipping and chirality-preserving terms become comparable as $m_\mu \sim m_s$.

The \tilde{U}_1 has only right-handed couplings. Therefore, it contributes only through the chirality-preserving terms. For $\kappa_Y = 1$, the \tilde{U}_1 leads to a positive Δa_μ . However, since the chirality-preserving contributions are proportional to m_μ^2 , one needs relatively larger values of x_1^{RR} to address the $(g-2)_\mu$ anomaly (this is true for vLQs with only left or right couplings in general).

B. Weak-doublet vector leptoquark

For a weak-doublet vLQ, the interaction and mass terms can be written as

$$\mathcal{L} \supset -\frac{1}{2}\text{Tr}[\vec{V}_{\mu\nu}^\dagger \vec{V}^{\mu\nu}] + M_V^2 \vec{V}_\mu^\dagger \vec{V}^\mu + ig_s \vec{V}_\mu^\dagger T_a \vec{V}_\nu \left(\kappa_s G_a^{\mu\nu} + \tilde{\kappa}_s \tilde{G}_a^{\mu\nu} \right) + ig' Y \vec{V}_\mu^\dagger \vec{V}_\nu \left(\kappa_Y B^{\mu\nu} + \tilde{\kappa}_Y \tilde{B}^{\mu\nu} \right) + ig \vec{V}_\mu^\dagger \frac{\tau_a}{2} \vec{V}_\nu \left(\kappa_w W_a^{\mu\nu} + \tilde{\kappa}_w \tilde{W}_a^{\mu\nu} \right). \quad (4)$$

It interacts with the electromagnetic field A^μ like the singlet vLQ [see Eq. (3)], except κ_Y and $\tilde{\kappa}_Y$ are replaced by effective couplings:

$$\kappa_{eff} = \frac{1}{Q} (Y \kappa_Y + T_3 \kappa_w), \quad \tilde{\kappa}_{eff} = \frac{1}{Q} (Y \tilde{\kappa}_Y + T_3 \tilde{\kappa}_w). \quad (5)$$

We set $\kappa_{eff} = 1$ and $\tilde{\kappa}_{eff} = 0$ in our calculations. As shown in Table I, two weak-doublet representations are possible: $V_2(\mathbf{\bar{3}}, \mathbf{2}, 5/6)$ and $\tilde{V}_2(\mathbf{\bar{3}}, \mathbf{2}, -1/6)$.

The interactions of the $V_2 = \{V_2^{4/3}, V_2^{1/3}\}$ (where the superscripts indicate the electric charges of the components)

¹ There, it is also pointed out that $\kappa_s = \kappa_Y = 1$ and $\tilde{\kappa}_s = \tilde{\kappa}_Y = 0$, in the

UV-complete models where the vLQ is the carrier of a spontaneously broken gauge symmetry. Otherwise, these parameters are free in general [43]. Since the dual terms are CP -violating, the nonzero $\tilde{\kappa}$ s parametrise additional sources of CP violation.

TABLE I. List of vLQs and their representations under the SM gauge groups. In the first column, the first and the second arguments within the parentheses indicate the representations under $SU(3)_c$ and $SU(2)_L$, respectively and the third argument is the hypercharge. The electric charge of a vLQ is given by $Q = T_3 + Y$ where T_3 is the third component of its isospin and Y is its hypercharge. We present the vLQ interactions in the up- and down-aligned scenarios for all vLQs [41, 44].

vLQ	Down-aligned vLQ interactions	Up-aligned vLQ interactions
$U_1 (3, 1, 2/3)$	$(Vx_1^{LL})_{ij} \bar{u}_L^i \gamma^\mu v_L^j U_{1,\mu} + (x_1^{LL})_{ij} \bar{d}_L^i \gamma^\mu e_L^j U_{1,\mu}$ $+ (x_1^{RR})_{ij} \bar{d}_R^i \gamma^\mu e_R^j U_{1,\mu}$	$(x_1^{LL})_{ij} \bar{u}_L^i \gamma^\mu v_L^j U_{1,\mu} + (V^\dagger x_1^{LL})_{ij} \bar{d}_L^i \gamma^\mu e_L^j U_{1,\mu}$ $+ (x_1^{RR})_{ij} \bar{d}_R^i \gamma^\mu e_R^j U_{1,\mu}$
$\tilde{U}_1 (3, 1, 5/3)$	$(\tilde{x}_1^{RR})_{ij} \bar{u}_R^i \gamma^\mu e_R^j \tilde{U}_1$	$(\tilde{x}_1^{RR})_{ij} \bar{u}_R^i \gamma^\mu e_R^j \tilde{U}_1$
$V_2 (\bar{3}, 2, 5/6)$	$-(x_2^{RL})_{ij} \bar{d}_R^i \gamma^\mu v_L^j V_{2,\mu}^{1/3} + (x_2^{RL})_{ij} \bar{d}_R^i \gamma^\mu e_L^j V_{2,\mu}^{4/3}$ $+ (V^* x_2^{LR})_{ij} \bar{u}_L^i \gamma^\mu e_R^j V_{2,\mu}^{1/3} - (x_2^{LR})_{ij} \bar{d}_L^i \gamma^\mu e_R^j V_{2,\mu}^{4/3}$	$-(x_2^{RL})_{ij} \bar{d}_R^i \gamma^\mu v_L^j V_{2,\mu}^{1/3} + (x_2^{RL})_{ij} \bar{d}_R^i \gamma^\mu e_L^j V_{2,\mu}^{4/3}$ $+ (x_2^{LR})_{ij} \bar{u}_L^i \gamma^\mu e_R^j V_{2,\mu}^{1/3} - (V^\dagger x_2^{LR})_{ij} \bar{d}_L^i \gamma^\mu e_R^j V_{2,\mu}^{4/3}$
$\tilde{V}_2 (\bar{3}, 2, -1/6)$	$-(\tilde{x}_2^{RL})_{ij} \bar{d}_R^i \gamma^\mu e_L^j \tilde{V}_2^{1/3} + (\tilde{x}_2^{RL})_{ij} \bar{u}_R^i \gamma^\mu v_L^j \tilde{V}_2^{-2/3}$	$-(\tilde{x}_2^{RL})_{ij} \bar{d}_R^i \gamma^\mu e_L^j \tilde{V}_2^{1/3} + (\tilde{x}_2^{RL})_{ij} \bar{u}_R^i \gamma^\mu v_L^j \tilde{V}_2^{-2/3}$
$U_3 (3, 3, 2/3)$	$-(x_3^{LL})_{ij} \bar{d}_L^i \gamma^\mu e_L^j U_{3,\mu}^{2/3} + (Vx_3^{LL})_{ij} \bar{u}_L^i \gamma^\mu v_L^j U_{3,\mu}^{2/3}$ $+ \sqrt{2}(x_3^{LL})_{ij} \bar{d}_L^i \gamma^\mu v_L^j U_{3,\mu}^{-1/3} + \sqrt{2}(Vx_3^{LL})_{ij} \bar{u}_L^i \gamma^\mu e_L^j U_{3,\mu}^{5/3}$	$-(V^\dagger x_3^{LL})_{ij} \bar{d}_L^i \gamma^\mu e_L^j U_{3,\mu}^{2/3} + (x_3^{LL})_{ij} \bar{u}_L^i \gamma^\mu v_L^j U_{3,\mu}^{2/3}$ $+ \sqrt{2}(V^\dagger x_3^{LL})_{ij} \bar{d}_L^i \gamma^\mu v_L^j U_{3,\mu}^{-1/3} + \sqrt{2}(x_3^{LL})_{ij} \bar{u}_L^i \gamma^\mu e_L^j U_{3,\mu}^{5/3}$

are shown in Table I. Both $V_2^{1/3}$ and $V_2^{4/3}$ contribute to a_μ (see Appendix A). Since $V_2^{4/3}$ has both left-handed and right-handed interactions, it can positively contribute to the chirality-flipping term in a_μ when the product $x_2^{LR} x_2^{RL}$ is positive. The $V_2^{1/3}$ component only gives a chirality-preserving positive contribution to a_μ .

The interactions for the $\tilde{V}_2 = \{\tilde{V}_2^{1/3}, \tilde{V}_2^{-2/3}\}$ are shown in Table I. Since $\tilde{V}_2^{-2/3}$ does not couple to muon, it is only the $\tilde{V}_2^{1/3}$ that contributes to a_μ . This contribution is always negative; hence, the \tilde{V}_2 can not explain the positive shift needed to explain the $(g-2)_\mu$ anomaly.

C. Weak-triplet vector leptoquark

The interactions and mass terms for a generic weak-triplet vLQ can be expressed as

$$\begin{aligned}
\mathcal{L} \supset & -\frac{1}{2} \text{Tr}[\vec{V}_{\mu\nu}^\dagger \vec{V}^{\mu\nu}] + M_V^2 \vec{V}_\mu^\dagger \vec{V}^\mu \\
& + i g_s \vec{V}_\mu^\dagger T_a \vec{V}_\nu \left(\kappa_s G_a^{\mu\nu} + \tilde{\kappa}_s \tilde{G}_a^{\mu\nu} \right) \\
& + i g' Y \vec{V}_\mu^\dagger \vec{V}_\nu \left(\kappa_Y B^{\mu\nu} + \tilde{\kappa}_Y \tilde{B}^{\mu\nu} \right) \\
& + i g \vec{V}_\mu^\dagger I^a \vec{V}_\nu \left(\kappa_w W_a^{\mu\nu} + \tilde{\kappa}_w \tilde{W}_a^{\mu\nu} \right), \quad (6)
\end{aligned}$$

where $I_{ij}^a = -i\epsilon_{ij}^a$ are the generators of the $SU(2)$ group in the adjoint representation. There is only one triplet vLQ species, $U_3(3, 3, 2/3)$, as shown in Table I.

Table I shows the interactions of the $U_3 = \{U_3^{5/3}, U_3^{-1/3}$ and $U_3^{2/3}\}$. Only $U_3^{2/3}$ and $U_3^{5/3}$ components contribute to a_μ . Since for $\kappa_{eff} = 1$ and $\tilde{\kappa}_{eff} = 0$, both contribute positively, they can lead to a positive shift in a_μ . However, in the absence of any chirality-flipping contribution, x_3^{LL} has to be large to explain the $(g-2)_\mu$ anomaly.

IV. FITTING THE $(g-2)_\ell$ MEASUREMENTS

We perform parameter scans to obtain the parameter regions consistent with the experimental values of $(g-2)_\ell$. The significant contributions come from the chirality-flipping terms that depend on the product of two independent couplings (which, in general, could be complex) as $\text{Re}(x_{i\ell}^{L\alpha} x_{i\ell}^{R\alpha*})$ [see Eq. (A2)]. Since the LHC only limits the absolute values of these couplings, we assume all couplings to be real for simplicity and vary the couplings within the perturbative range, i.e., $[-\sqrt{4\pi}, \sqrt{4\pi}]$. In most plots, however, we do not show the entire range but focus only on the interesting parts.

We list the vLQs that can, in principle, provide a positive shift to $(g-2)_\mu$, i.e., $\Delta a_\mu > 0$ in the limit $\kappa_Y = 1$, $\tilde{\kappa}_Y = 0$ (or $\kappa_{eff} = 1$, $\tilde{\kappa}_{eff} = 0$) in Table II. However, if we take a bottom-up minimalist point of view in terms of the number of new vLQ couplings, we find that no vLQ can explain the $(g-2)_\mu$ anomaly with just one coupling of $\mathcal{O}(1)$ or smaller (while the rest are practically zero or negligible). Table III shows the ranges of the individual couplings needed to accommodate the $(g-2)_\ell$ measurements at 1σ level for $M_{\ell_q} = 2.5$ TeV. With just one coupling, only the chirality-preserving term contributes. Since it is sup-

TABLE II. vLQs that can produce the necessary Δa_ℓ in the single-coupling scenarios. However, in all the single coupling scenarios, the values of the couplings exceed the perturbative limit (see Table III). For U_1 and V_2 , the \checkmark in parenthesis indicates that the necessary Δa_ℓ value can be achieved in two-coupling scenarios with perturbative couplings through chirality-flipping terms (see Table III and Figs. 2 and 3).

	U_1	\tilde{U}_1	V_2	\tilde{V}_2	U_3
Δa_μ	$\checkmark (\checkmark)$	\checkmark	$\times (\checkmark)$	\times	\checkmark
Δa_e^{Rb}	$\checkmark (\checkmark)$	\checkmark	$\times (\checkmark)$	\times	\checkmark
Δa_e^{Cs}	$\times (\checkmark)$	\times	$\checkmark (\checkmark)$	\checkmark	\times

pressed by $m_\mu^2/M_{\ell_q}^2$, the associated coupling must be pretty large to explain the anomaly. The coupling can be lower for lighter vLQs; however, since the current bounds on vLQ masses from the direct pair-production searches are roughly about 2 TeV, the vLQs cannot be much lighter. On the other hand, increasing the mass would only push the coupling to a bigger value beyond the perturbative regime.

Only U_1 and V_2 can accommodate the $(g-2)_\mu$ anomaly with two non-negligible couplings through the chirality-flipping term ($\sim m_q m_\mu$) (see Table IV). There are three possible two-coupling scenarios for the three generations of quarks. For the third-generation quarks, the chirality-flipping term dominates, but for the lighter quarks, the chirality-preserving term dominates. Hence, in the $\{x_{32}^{LL}, x_{32}^{RR}\}$ scenario for U_1 and the $\{x_{32}^{LR}, x_{32}^{RL}\}$ scenario for V_2 , the couplings are much smaller than the light-quark couplings to address the $(g-2)_\mu$ anomaly. (Since now we focus only on U_1 and V_2 , we suppress the subscript indicating the vLQ representations from the couplings, as it is clear from the context; see Table D). Among the up- and down-aligned scenarios, the up-aligned x_{32} scenarios for U_1 and V_2 can contribute to the $R_K^{(*)}$ observable through quark mixing. Since the $R_K^{(*)}$ in the SM is a loop-induced process, but vLQs contribute at the tree level, the $R_K^{(*)}$ measurements eliminate almost the entire parameter space. This makes the up-aligned x_{32} scenarios for U_1 and V_2 very restrictive. Hence, we do not consider them further in our analysis.

If we consider the electron couplings instead of the muon, we get the vLQ contributions to electron AMDM. As mentioned earlier, Δa_e^{Rb} is positive whereas Δa_e^{Cs} is negative. Hence, essentially U_1 , \tilde{U}_1 , and U_3 can accommodate the Δa_e^{Rb} measurement; whereas parameter regions consistent with the Δa_e^{Cs} measurement can only be found for V_2 and \tilde{V}_2 (see Table II)—there are no common overlapping regions. We show the preferred coupling ranges for scenarios with one electron coupling and two electron couplings obtained using Δa_e^{Rb} and Δa_e^{Cs} measurements. For two couplings, the allowed coupling values are small when vLQs are connected with the first- and second-generation quarks. Therefore, these scenarios may agree with the LHC data.

As discussed in Sec. II, the current sensitivity on the measurements of a_τ is poor. Therefore, the experimental measurements of a_τ cannot set any significant limit on the vLQ parameter space. In the future, if the sensitivity on a_τ improves to $\sim 10^{-6}$, one might constrain vLQ couplings within the perturbative range especially involving third-generation quarks. A similar analysis for scalar LQ has been performed in Ref. [45].

V. LHC CONSTRAINTS AND RESULTS

It is well-known that the high-energy LHC data strongly constrain the parameter spaces of vLQs, especially in large-coupling limits. Because of the relatively larger parton density functions (PDFs) of the light quarks, the LHC constraints on vLQ couplings are particularly stringent when the vLQs interact with the first- and second-generation

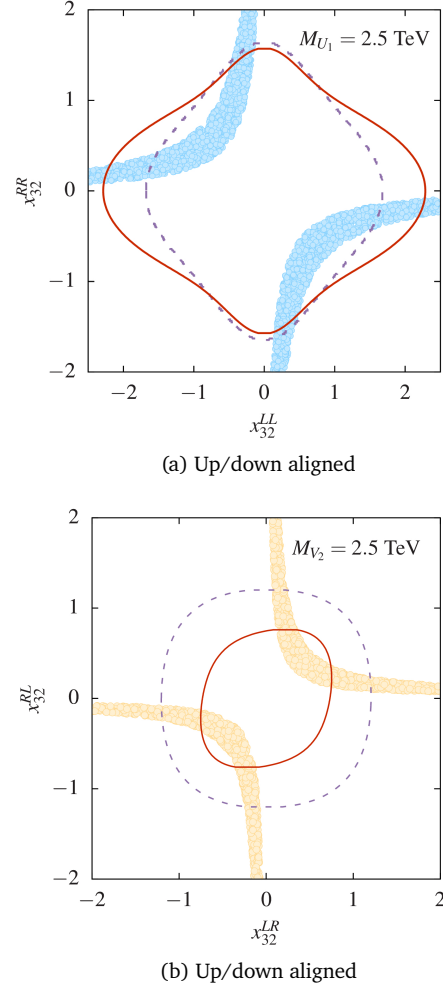


FIG. 2. U_1 and V_2 2σ $(g-2)_\mu$ parameter spaces and the corresponding LHC direct search (solid) and indirect dilepton (dashed) bounds. The regions inside the bounds are allowed. The difference between the up- and down-aligned scenarios can be seen from Table I.

quarks [21]. On the other hand, as Tables III and IV indicate, large couplings are required to satisfy the observed shift in a_μ . Consequently, there is no overlap between the $(g-2)_\mu$ parameter regions and those allowed by the LHC data. However, when vLQs couple with third-generation quarks, overlapping regions open up.

We briefly discuss how one can recast the LHC data to constrain the LQ parameter space [22]. The LHC limits are of two types—direct (mainly from the LQ pair production searches in the dilepton-dijet channels [46]) and indirect (from the dilepton resonance searches [47]).

- (a) *Dilepton-dijet ($\ell\ell jj$) data:* the current limit on vLQ mass from the pair-production searches is around 2 TeV for 100% decay in the search mode. The limits weaken when the branching ratio (BR) in the search mode goes down in scenarios with multiple couplings. However, as illustrated in Ref. [22] (earlier in Refs. [23, 48] in related contexts), other production processes—such as single productions, indirect productions (t -channel vLQ exchanges and their interference with SM processes)—can also contribute

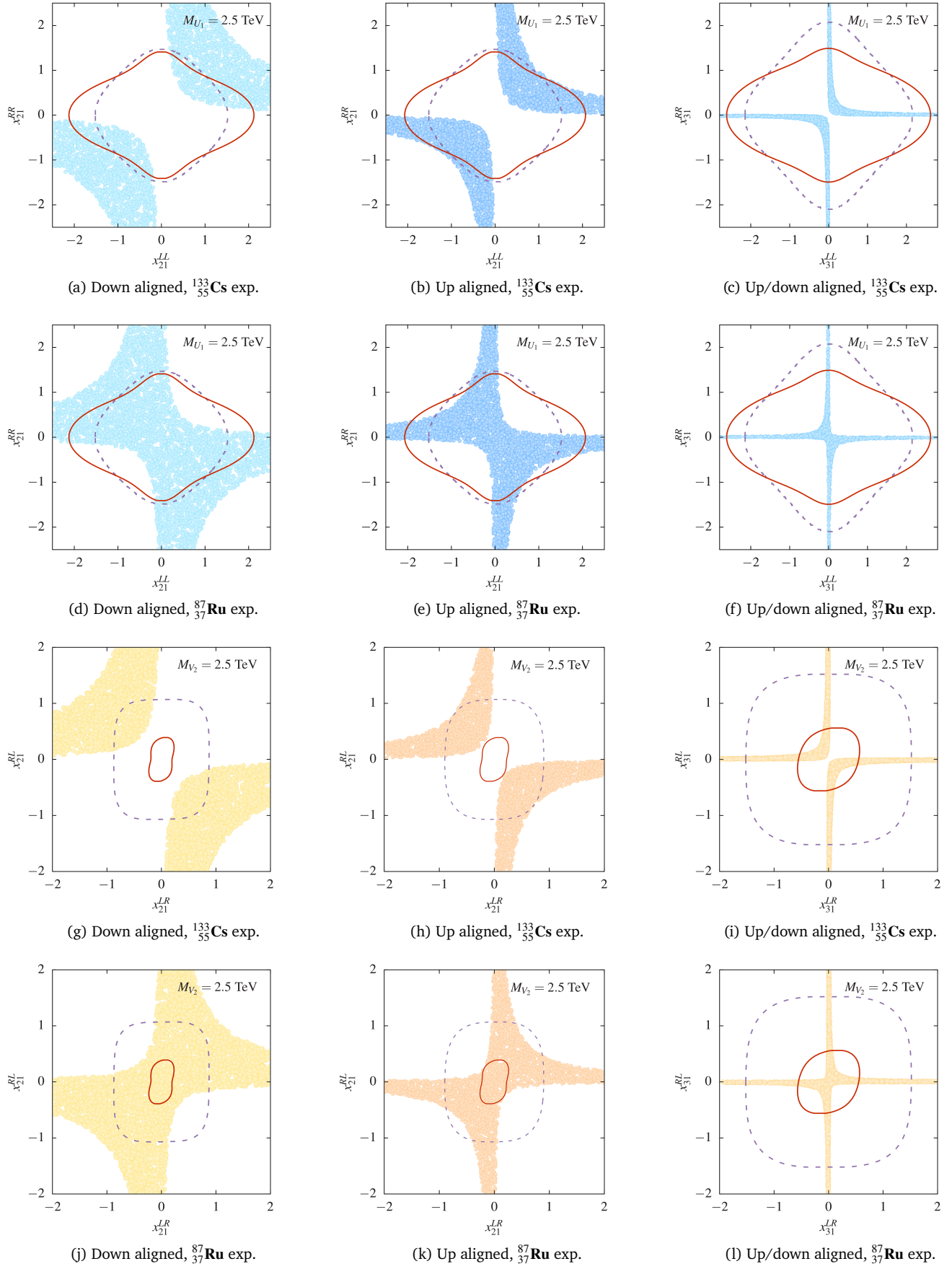


FIG. 3. Same as Fig. 2 except for the electron instead of the muon.

TABLE III. Summary of the bounds on the vLQ couplings (listed in Table I) contributing to the AMDMs of the electron and muon through the chirality-preserving term [$\sim m_\ell^2/M_{\ell_q}^2$, see Eq. (A2)], considering each coupling separately (single-coupling scenarios). These are 1σ bounds on the absolute values of the couplings for $M_{\ell_q} = 2.5$ TeV.

vLQ	Couplings	Q_q	From Δa_μ	From Δa_e^{Cs}	Form Δa_e^{Ru}
$U_1^{2/3}$	$ x_{1\ell}^{LL} , x_{1\ell}^{RR} $	$-\frac{1}{3}$	[6.18, 7.62]	—	[12.56, 25.77]
$\tilde{U}_1^{5/3}$	$ x_{1\ell}^{RR} $	$\frac{2}{3}$	[5.65, 7.10]	—	[11.25, 23.40]
$V_2^{1/3}, V_2^{4/3}$	$ x_{2\ell}^{LR} , x_{2\ell}^{RL} $	$\frac{2}{3}, -\frac{1}{3}$	—	[17.20, 26.73]	—
$\tilde{V}_2^{1/3}$	$ x_{2\ell}^{RL} $	$\frac{2}{3}$	—	[26.04, 40.75]	—
$U_3^{2/3}$	$ x_{3\ell}^{LL} $	$-\frac{1}{3}$	[3.30, 4.11]	—	[6.65, 14.15]

TABLE IV. Similar to Table III but for product of couplings in the U_1 and V_2 up- and down-aligned two-coupling scenarios. In these scenarios, the chirality-flipping term [$\sim m_\ell m_q/M_{\ell_q}^2$, see Eq. (A2)] contributes dominantly.

vLQ	Coupling products	Alignment	From Δa_μ	From Δa_e^{Cs}	From Δa_e^{Ru}
U_1	$x_{3\ell}^{LL} x_{3\ell}^{RR}$	up	[-0.55, -0.37]	[0.02, 0.04]	[-0.03, -0.007]
		down	[-0.55, -0.37]	[0.02, 0.05]	[-0.03, -0.007]
	$x_{2\ell}^{LL} x_{2\ell}^{RR}$	up	[-8.70, -5.88]	[0.31, 0.77]	[-0.50, -0.11]
		down	[-24.35, -16.45]	[0.88, 2.14]	[-1.40, -0.31]
	$x_{1\ell}^{LL} x_{1\ell}^{RR}$	up	[-56.67, -38.30]	[2.13, 5.07]	[-3.20, -0.73]
		down	[-488.0, -329.0]	[18.0, 43.4]	[-27.7, -6.4]
	$x_{3\ell}^{LR} x_{3\ell}^{RL}$	up	[0.22, 0.33]	[-0.03, -0.01]	[0.004, 0.018]
		down	[0.22, 0.33]	[-0.03, -0.01]	[0.004, 0.018]
V_2	$x_{2\ell}^{LR} x_{2\ell}^{RL}$	up	[3.54, 5.31]	[-0.46, -0.19]	[0.06, 0.30]
		down	[9.87, 14.80]	[-1.30, -0.54]	[0.18, 0.80]
	$x_{1\ell}^{LR} x_{1\ell}^{RL}$	up	[23.40, 34.12]	[-2.96, -1.26]	[0.43, 1.86]
		down	[201.52, 296.65]	[-26.0, -11.0]	[3.80, 16.11]

to the $\ell\ell jj$ final states. These additional contributions become significant for order-one vLQ couplings, leading to stronger mass exclusion bounds. We obtain the recast direct limits relevant to our study following the method explained in Ref. [22].

- (b) *Dilepton ($\ell\ell$) resonance data:* all the above-mentioned production processes also contribute to the $\ell\ell$ resonance-search signals and affect the high- p_T tails of the dilepton distributions. The t -channel vLQ exchange process can significantly interfere with the SM background ($q\bar{q} \rightarrow Z/\gamma^* \rightarrow \ell^+\ell^-$). For example, in the presence of muon couplings, vLQs produced at the LHC would contribute to the $\mu\mu(+X)$ final state and affect the high- p_T tail of the dimuon distribution observed at the LHC. One can fit the observed dimuon invariant mass distribution from Ref. [47] with vLQ events and estimate the limits on the coupling(s) using the χ^2 estimation technique.

The method explained in Ref. [21] (also see [20]) is easily extendable to scenarios with multiple new couplings. In this paper, we use an automated implementation of this method [49] to locate the region(s) of parameter space allowed by the LHC data in each scenario we consider. In the automated implementation, the vLQ interactions are first implemented in FEYNRULES [50] to create the Universal FeynRules Output [51] model files for MADGRAPH [52]. PYTHIA8 [53] performs parton showering and hadronization on the events generated in MADGRAPH. The detector simulation is performed with DELPHES [54]. (We use the same computational setup to estimate the direct limits.)

For 2.5 TeV U_1 and V_2 , we show how the direct and indirect LHC bounds constrain large values of the couplings on two-couplings planes. In Fig. 2(a), we show the parameter ranges in the $\{x_{32}^{LL}, x_{32}^{RR}\}$ up-/down-aligned U_1 sce-

narios that can address the $(g-2)_\mu$ anomaly. These two-coupling scenarios of U_1 can address the a_μ discrepancy with perturbative couplings, as shown in Table IV. The indirect limit is stronger than the direct one along x_{32}^{LL} , as the latter is more sensitive to the reduction in $\text{BR}(U_1 \rightarrow \mu b)$ (x_{32}^{LL} lets the U_1 decay via $U_1 \rightarrow \nu b$ mode). Fig. 2(a) shows similar LHC bounds/ $(g-2)_\mu$ -favoured parameter ranges on the $\{x_{32}^{LR}, x_{32}^{RL}\}$ plane for V_2 . In this case, unlike for the U_1 , the couplings are positively correlated, and the direct bounds are tighter and severely restrict the viable parameter ranges. We show the corresponding plots for electron AMDM measurements with $^{133}_{55}\text{Cs}$ and $^{87}_{37}\text{Ru}$ in Fig. 3. There, we also show the LHC bounds on the scenarios with second-generation quark couplings, i.e., $\{x_{21}^{XX}, x_{31}^{XX}\}$. We see that good parts of the U_1 parameter space survive the LHC bounds but for V_2 , the LHC data completely rule out the $\{x_{21}^{LR}, x_{31}^{RL}\}$ up-/down-aligned scenarios preferred by the $^{133}_{55}\text{Cs}$ measurement.

VI. ELECTRIC DIPOLE MOMENT

So far, we have assumed all couplings to be real. With this assumption, vLQs contribute to the lepton AMDMs but not their EDMs [as we set $\tilde{\kappa}_\alpha = 0$, see Eq. (A3)]. If we relax this restriction and allow the couplings to have imaginary parts, the main chirality-flipping term in d_ℓ , which is proportional to $\text{Im}(x_{3\ell}^{L\alpha} x_{i\ell}^{R\bar{\alpha}*})$, starts contributing. To give some idea about the EDM limits, we consider a benchmark set of values for $x_{3\ell}^{LL}$ and $\text{Re}(x_{3\ell}^{RR})$ consistent with the Δa_ℓ measurements and the LHC bounds for a 2.5 TeV U_1 in Table V. The last column shows that the current experimental value of d_e forces the imaginary part of the x_{31}^{RR} coupling to be tiny.

TABLE V. Limits on the imaginary couplings of a 2.5 TeV U_1 from the current measurements of the EDM of the electron and the neutron (for μ and τ). We assume one of the couplings ($x_{3\ell}^{LL}$) to be real. The real part of the other coupling ($x_{3\ell}^{RR}$) is chosen to satisfy the AMDM measurements and the LHC bounds. The limits are obtained for the best-fit value of $\beta_n^{\tilde{G}} \approx 2 \times 10^{-20} \text{e cm}$ [see Eq. (7)].

Lepton	Benchmark choice		Upper limit
	$x_{3\ell}^{LL}$	$\text{Re}(x_{3\ell}^{RR})$	$\text{Im}(x_{3\ell}^{RR})$
e ($^{133}_{55}\text{Cs}$)	$0.5 + 0i$	0.06	$5 \times 10^{-8} (d_e)$
e ($^{87}_{37}\text{Ru}$)	$0.5 + 0i$	-0.06	$5 \times 10^{-8} (d_e)$
μ	$0.5 + 0i$	1	$94.5 (d_n)$
τ	$0.5 + 0i$	0	$5.5 (d_n)$

TABLE VI. Limits on the vLQ couplings for 2.5 TeV U_1 and V_2 from the APV measurement of the $^{133}_{55}\text{Cs}$ nucleus.

	Couplings	U_1	Couplings	V_2
	x_{11}^{LL}	\times	x_{11}^{LR}	\times
1σ	x_{11}^{RR}	$[0.21, 0.67]$	x_{11}^{RL}	$[0.21, 0.67]$
2σ	x_{11}^{LL}	$[0, 0.40]$	x_{11}^{LR}	$[0, 0.30]$
	x_{11}^{RR}	$[0, 0.78]$	x_{11}^{RL}	$[0, 0.80]$

However, similar constraints from the d_μ and d_τ measurements are weak—they go beyond the perturbative range. Instead, we show the bounds from the neutron EDM (d_n) measurements [55], which, as shown in Ref. [10], are relatively tighter in these cases but, nevertheless, not very restrictive. The dominant U_1 contribution to d_n can be expressed as [10]

$$d_n^{\tilde{G}} \approx -\frac{g_s^3 v^2}{(16\pi^2)^2 m_b M_{U_1}^2} \beta_n^{\tilde{G}} \sum_{\ell} m_{\ell} \text{Im}(x_{3\ell}^{LX} x_{3\ell}^{RY*}), \quad (7)$$

where $\beta_n^{\tilde{G}} \approx [0.2, 40] \times 10^{-20} \text{e cm}$ [56] is the nucleon matrix element. For V_2 and other vLQs, the limits are similar. Hence, we do not discuss EDM limits further (interested readers can see Ref. [57]).

VII. ATOMIC PARITY VIOLATION

The APV measurement in the $^{133}_{55}\text{Cs}$ nucleus constrains the vLQ interactions with the first-generation fermions. The tree-level vLQ contribution can be parameterised as follows [41]:

$$\mathcal{L} = \frac{G_F}{\sqrt{2}} \bar{e} \gamma^\mu \gamma^5 e (\delta C_{1u} \bar{u} \gamma_\mu u + \delta C_{1d} \bar{d} \gamma_\mu d), \quad (8)$$

where δC_{1u} and δC_{1d} come from vLQs. The U_1 only contributes to δC_{1d} as it cannot simultaneously couple to the up quark and the electron. The δC_{1d} from U_1 is given as

$$\delta C_{1d}^{U_1} = \frac{v^2}{2M_{U_1}^2} |x_{11}^{LL}|^2 - \frac{v^2}{2M_{U_1}^2} |x_{11}^{RR}|^2, \quad (9)$$

where v is the Higgs vacuum expectation value. For V_2 , δC_{1u} and δC_{1d} take the following forms:

$$\begin{aligned} \delta C_{1u}^{V_2} &= \frac{v^2}{2M_{V_2}^2} |x_{11}^{LR}|^2, \\ \delta C_{1d}^{V_2} &= \frac{v^2}{2M_{V_2}^2} |x_{11}^{LR}|^2 - \frac{v^2}{2M_{V_2}^2} |x_{11}^{RL}|^2. \end{aligned} \quad (10)$$

The above coefficients modify the weak charge for the $^{133}_{55}\text{Cs}$ nucleus as:

$$\delta Q_W^{\text{Cs}} = -2(188 \delta C_{1u} + 211 \delta C_{1d}) \quad (11)$$

From experiments, we have $Q_W^{\text{Cs}}(\text{exp}) = -72.82 \pm 0.42$ [32] and $Q_W^{\text{Cs}}(\text{SM}) = -73.33$, where the SM values are, $C_{1u}^{\text{SM}} = -0.1887$ and $C_{1d}^{\text{SM}} = 0.3419$ [58]. In Table VI, we summarise the limits on the vLQ couplings obtained from the APV measurements for $M_{\ell q} = 2.5 \text{ TeV}$. The entire 1σ range of the δQ_W^{Cs} is positive, $[0.09, 0.93]$ whereas the 2σ range stretches from negative to positive values, $[-0.33, 1.35]$. This is why we can rule out x_{11}^{LL} (for U_1) and x_{11}^{LR} (for V_2) single coupling scenarios for the 1σ range of δQ_W^{Cs} .

VIII. SUMMARY AND CONCLUSIONS

In this paper, we examined the contributions of vLQs to the dipole moments of charged leptons—particularly e and μ ,

TABLE VII. Illustrative Feynman rules and momentum conventions.

Diagram	Rule	Diagram	Rule
	$x^{LL}\Gamma_\mu$		$x^{RR}\Gamma_\mu$
	$x^{LR}\Gamma_\mu$		$x^{RL}\Gamma_\mu$
	γ_μ		$-\gamma_\mu$
	$\mathcal{P}_{\mu,\alpha,\beta} = (\kappa_Y p_{3\beta} - p_{1\beta})g_{\mu\alpha} - (\kappa_Y p_{3\alpha} - p_{2\alpha})g_{\mu\beta} + (p_{1\mu} - p_{2\mu})g_{\beta\alpha} + \tilde{\kappa}_Y \epsilon_{\mu\alpha\beta\delta} p_3^\delta$		
	$V^{\mu\nu}(p) = \frac{1}{p^2 - M_V^2} \left(g^{\mu\nu} - \frac{p^\mu p^\nu}{M_V^2} \right)$		
			$S(p) = \frac{i(\not{p} + m)}{p^2 - m^2}$
			$S(p) = \frac{i(-\not{p} + m)}{p^2 - m^2}$

which are measured precisely—in light of the high-energy dilepton data from the LHC. We derived the contributions of weak-singlet, doublet, and triplet vLQs to $(g-2)_\ell$ in the presence of additional gauge couplings κ and $\tilde{\kappa}$. The parameter space favoured by the $(g-2)_\ell$ measurements is constrained by the LHC dilepton bounds. Following the method outlined in Ref. [22], we considered both the dilepton-dijet and the dilepton resonance search data to derive the LHC bounds. In the parameter range of our interest, the LHC limits dominantly come from the t -channel vLQ-exchange diagrams and their interference with the SM background, making the LHC constraints insensitive to κ and $\tilde{\kappa}$. We set $\kappa = 1$ and $\tilde{\kappa} = 0$ throughout our analysis, as the one-loop vLQ contributions to leptonic dipole moments remain independent of the loop-momentum cut-off in this limit. In this limit, our results also agree with Ref. [10].

In single-coupling scenarios, $(g-2)_\ell$ gets contributions from chirality-preserving terms that are suppressed by $m_\ell^2/M_{\ell_q}^2$. Consequently, no single-coupling scenario can ac-

count for the measured $(g-2)_\ell$ values for perturbative couplings. However, vLQs that couple to both left- and right-handed leptons can resolve the $(g-2)_\mu$ anomaly through chirality-flipping contributions in principle. Of the five possible vLQs, this is only possible for U_1 and V_2 . These two vLQs can explain the observed positive shift in Δa_μ with perturbative couplings in two-coupling scenarios, provided they interact with third-generation quarks, as is the case in the down-aligned x_{32}^{LX}, x_{32}^{RY} scenarios ($\{X, R\} = \{L, R\}$ for U_1 and $\{X, Y\} = \{R, L\}$ for V_2). One could, in principle, consider similar up-aligned scenarios as well. However, those will contribute significantly to a range of observables in meson mixings ($B_0-\bar{B}_0$, $B_s-\bar{B}_s$, $K_0-\bar{K}_0$, etc.) and decays ($R_{K^{(*)}}, R_{K^{(*)}}^V$, $B_s \rightarrow \mu\mu$, etc.). (The down-aligned scenarios also contribute to $D_0-\bar{D}_0$ mixing and decays such as $D_0 \rightarrow \mu\mu$ and $B \rightarrow \mu\nu$, but off-diagonal Cabibbo-Kobayashi-Maskawa matrix elements strongly suppress the contributions.) The Z-boson decays also constrain these scenarios (see, e.g., Ref. [59] for a similar case with scalar LQs) but the dominant contributions from the top-quark

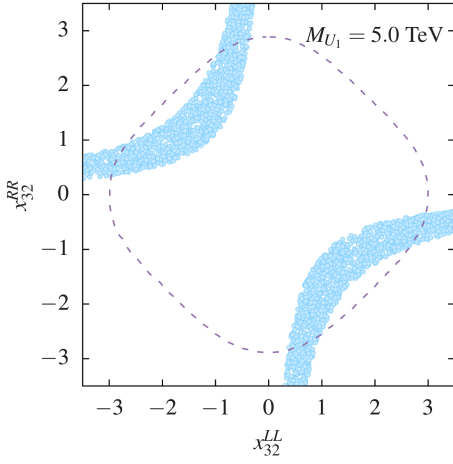


FIG. 4. Case of heavy vLQs: an illustration with 5 TeV U_1 —the $(g-2)_\mu$ parameter space and the corresponding indirect LHC bound. For heavy vLQs, the indirect bounds are more restrictive than the direct ones. Compared to Fig. 2, the necessary couplings have increased, but the LHC limit has also loosened.

loops are absent in the down-aligned scenarios. While it is certainly interesting to investigate the role of various low-energy bounds in different scenarios, a comprehensive analysis lies beyond the scope of this paper.

The AMDM measurements for electrons show a mild discrepancy, with conflicting results between the $^{133}_{55}\text{Cs}$ -based and $^{87}_{37}\text{Rb}$ -based experiments. We found that two-coupling (chirality-flipping) scenarios can account for the measured values of $(g-2)_e$, yielding perturbative coupling solutions, especially when the vLQs couple to either second- or third-generation quarks. We performed parameter scans for 2.5 TeV U_1 and V_2 to show how these vLQs can accommodate the precisely measured AMDMs of the electron and the muon without conflicting with the LHC bounds. The LHC bounds prevent these vLQs from being much lighter than $\sim (2-2.5)$ TeV. On the other hand, since heavier vLQs require large couplings to accommodate the $(g-2)_\ell$ measurements (see Fig. 4, which shows the trend), they cannot be arbitrarily heavy if we demand the couplings remain in the perturbative domain. For example, for $x_{32}^{LL}x_{32}^{RR} < \sqrt{16\pi^2}$, the U_1 cannot be heavier than about 13 TeV. Similarly, for $x_{32}^{LR}x_{32}^{RL} < \sqrt{16\pi^2}$, $M_{V_2} \lesssim 17$ TeV. However, such heavy vLQs will be much beyond the direct reach of the current collider experiments.

If we assume the new couplings are complex in general, vLQs contribute to lepton EDMs. However, except for the electron, the current lepton EDM measurements are too weak to restrict the μ and τ couplings within the perturbative range (which are ruled out by the LHC data anyway). Only the electron EDM measurement can put a tight bound on the imaginary parts of the electron couplings if we assume $\tilde{\kappa} = 0$. The electron couplings with the first-generation quarks are also constrained to be within the perturbative range by the APV measurements.

ACKNOWLEDGEMENT

We thank Arijit Das for helping us with the direct LHC limits. D.D. would like to thank the SERB/ANRF, Govt. of India for the SRG Grant Order No. SRG/2023/001318 and IIIT Hyderabad for the Seed Grant No. IIIT/R&D Office/Seed-Grant/2021-22/013. T.M. is supported by the intramural grant from IISER-TVM.

Appendix A: Anomalous magnetic-dipole moment of leptons in vLQ scenarios

The general lagrangian for a $SU(2)_L$ -singlet, -doublet, or -triplet vLQ interaction with the SM quarks and charged leptons can be written as

$$\mathcal{L} \supset x_{ij}^{LL} \bar{q}_L^i \gamma_\mu \ell_L^j V_0^\mu + x_{ij}^{RR} \bar{q}_R^i \gamma_\mu \ell_R^j V_0^\mu + x_{ij}^{RL} \bar{q}_R^i \gamma_\mu \ell_L^j V_2^\mu + x_{ij}^{LR} \bar{q}_L^i \gamma_\mu \ell_R^j V_2^\mu + h.c. \quad (\text{A1})$$

With this, the generic vLQ contribution to a_ℓ at the leading order can be written as

$$a_\ell = \frac{N_c}{16\pi^2} \sum_{i=1}^3 \sum_{\alpha}^{L,R} \left[2\text{Re}(x_{i\ell}^{L\alpha} x_{i\ell}^{R\bar{\alpha}*}) \frac{m_\ell m_{q_i}}{M_{\ell_q}^2} \left\{ 2Q_q + Q_{\ell_q} \left((1 - \kappa_\alpha) \ln \left(\frac{\Lambda^2}{M_{\ell_q}^2} \right) + \frac{1 - 5\kappa_\alpha}{2} \right) \right\} + (1 - 2\delta_{L\alpha}) (|x_{i\ell}^{L\alpha}|^2 + |x_{i\ell}^{R\bar{\alpha}}|^2) \frac{m_\ell^2}{M_{\ell_q}^2} \left\{ \frac{4}{3} Q_q + Q_{\ell_q} \left((1 - \kappa_\alpha) \ln \left(\frac{\Lambda^2}{M_{\ell_q}^2} \right) - \frac{1 + 9\kappa_\alpha}{6} \right) \right\} + 2\tilde{\kappa}_\alpha Q_{\ell_q} \text{Im}(x_{i\ell}^{L\alpha} x_{i\ell}^{R\bar{\alpha}*}) \frac{m_\ell m_{q_i}}{M_{\ell_q}^2} \left(\ln \frac{\Lambda^2}{M_{\ell_q}^2} - \frac{1}{2} \right) \right], \quad (\text{A2})$$

where $\bar{\alpha}$ stands for the opposite chirality to α , $\kappa_\alpha = \kappa_Y$ and $\tilde{\kappa}_\alpha = \tilde{\kappa}_Y$ if $\alpha = L$ (e.g., for singlet vLQs), and $\kappa_\alpha = \kappa_{eff}$ and $\tilde{\kappa}_\alpha = \tilde{\kappa}_{eff}$ otherwise (i.e., for doublet vLQs). Similarly, the contribution to d_ℓ can be written as

$$d_\ell = \frac{eN_c}{16\pi^2} \sum_{i=1}^3 \sum_{\alpha}^{L,R} \left[\text{Im}(x_{i\ell}^{L\alpha} x_{i\ell}^{R\bar{\alpha}*}) \frac{m_{q_i}}{M_{\ell_q}^2} \left\{ 2Q_q + Q_{\ell_q} \left((1 - \kappa_\alpha) \ln \left(\frac{\Lambda^2}{M_{\ell_q}^2} \right) + \frac{1 - 5\kappa_\alpha}{2} \right) \right\} + (2\delta_{L\alpha} - 1) Q_{\ell_q} \tilde{\kappa}_\alpha (|x_{i\ell}^{L\alpha}|^2 + |x_{i\ell}^{R\bar{\alpha}}|^2) \frac{m_\ell}{M_{\ell_q}^2} \left(\frac{1}{2} \ln \frac{\Lambda^2}{M_{\ell_q}^2} - \frac{3}{4} \right) - \tilde{\kappa}_\alpha Q_{\ell_q} \text{Re}(x_{i\ell}^{L\alpha} x_{i\ell}^{R\bar{\alpha}*}) \frac{m_{q_i}}{M_{\ell_q}^2} \left(\ln \frac{\Lambda^2}{M_{\ell_q}^2} - \frac{1}{2} \right) \right]. \quad (\text{A3})$$

We evaluate the loop contributions following the convention in Table VII and using PACKAGE-X [60] in the limit $m_\mu, m_q \ll M_{\ell_q}$, where m_q and M_{ℓ_q} are the masses of the quark and the vLQ in the loop.

- [1] S. Navas *et al.* (Particle Data Group), “Review of particle physics,” *Phys. Rev. D* **110**, 030001 (2024).
- [2] T. Aoyama *et al.*, “The anomalous magnetic moment of the muon in the Standard Model,” *Phys. Rept.* **887**, 1–166 (2020), [arXiv:2006.04822 \[hep-ph\]](#); Tatsumi Aoyama, Masashi Hayakawa, Toichiro Kinoshita, and Makiko Nio, “Complete Tenth-Order QED Contribution to the Muon $g-2$,” *Phys. Rev. Lett.* **109**, 111808 (2012), [arXiv:1205.5370 \[hep-ph\]](#); Tatsumi Aoyama, Toichiro Kinoshita, and Makiko Nio, “Theory of the Anomalous Magnetic Moment of the Electron,” *Atoms* **7**, 28 (2019); Andrzej Czarnecki, William J. Marciano, and Arkady Vainshtein, “Refinements in electroweak contributions to the muon anomalous magnetic moment,” *Phys. Rev. D* **67**, 073006 (2003), [Erratum: *Phys. Rev. D* **73**, 119901 (2006)], [arXiv:hep-ph/0212229 \[hep-ph\]](#); C. Gnendiger, D. Stöckinger, and H. Stöckinger-Kim, “The electroweak contributions to $(g-2)_\mu$ after the Higgs boson mass measurement,” *Phys. Rev. D* **88**, 053005 (2013), [arXiv:1306.5546 \[hep-ph\]](#); Kirill Melnikov and Arkady Vainshtein, “Hadronic light-by-light scattering contribution to the muon anomalous magnetic moment revisited,” *Phys. Rev. D* **70**, 113006 (2004), [arXiv:hep-ph/0312226 \[hep-ph\]](#); Pere Masjuan and Pablo Sánchez-Puertas, “Pseudoscalar-pole contribution to the $(g_\mu - 2)$: a rational approach,” *Phys. Rev. D* **95**, 054026 (2017), [arXiv:1701.05829 \[hep-ph\]](#); Gilberto Colangelo, Martin Hoferichter, Massimiliano Procura, and Peter Stoffer, “Dispersion relation for hadronic light-by-light scattering: two-pion contributions,” *JHEP* **04**, 161 (2017), [arXiv:1702.07347 \[hep-ph\]](#); Martin Hoferichter, Bai-Long Hoid, Bastian Kubis, Stefan Leupold, and Sebastian P. Schneider, “Dispersion relation for hadronic light-by-light scattering: pion pole,” *JHEP* **10**, 141 (2018), [arXiv:1808.04823 \[hep-ph\]](#); Antoine Gérardin, Harvey B. Meyer, and Andreas Nyffeler, “Lattice calculation of the pion transition form factor with $N_f = 2 + 1$ Wilson quarks,” *Phys. Rev. D* **100**, 034520 (2019), [arXiv:1903.09471 \[hep-lat\]](#); Johan Bijnens, Nils Hermansson-Truedsson, and Antonio Rodríguez-Sánchez, “Short-distance constraints for the HLbL contribution to the muon anomalous magnetic moment,” *Phys. Lett. B* **798**, 134994 (2019), [arXiv:1908.03331 \[hep-ph\]](#); Gilberto Colangelo, Franziska Hagelstein, Martin Hoferichter, Laetitia Laub, and Peter Stoffer, “Longitudinal short-distance constraints for the hadronic light-by-light contribution to $(g-2)_\mu$ with large- N_c Regge models,” *JHEP* **03**, 101 (2020), [arXiv:1910.13432 \[hep-ph\]](#); Thomas Blum, Norman Christ, Masashi Hayakawa, Taku Izubuchi, Luchang Jin, Chulwoo Jung, and Christoph Lehner, “The hadronic light-by-light scattering contribution to the muon anomalous magnetic moment from lattice QCD,” *Phys. Rev. Lett.* **124**, 132002 (2020), [arXiv:1911.08123 \[hep-lat\]](#); Gilberto Colangelo, Martin Hoferichter, Andreas Nyffeler, Massimo Passera, and Peter Stoffer, “Remarks on higher-order hadronic corrections to the muon $g-2$,” *Phys. Lett. B* **735**, 90–91 (2014), [arXiv:1403.7512 \[hep-ph\]](#).
- [3] Michel Davier, Andreas Hoecker, Bogdan Malaescu, and Zhiqing Zhang, “Reevaluation of the hadronic vacuum polarisation contributions to the Standard Model predictions of the muon $g-2$ and $\alpha(m_Z^2)$ using newest hadronic cross-section data,” *Eur. Phys. J. C* **77**, 827 (2017), [arXiv:1706.09436 \[hep-ph\]](#); Alexander Keshavarzi, Daisuke Nomura, and Thomas Teubner, “Muon $g-2$ and $\alpha(m_Z^2)$: a new data-based analysis,” *Phys. Rev. D* **97**, 114025 (2018), [arXiv:1802.02995 \[hep-ph\]](#); Gilberto Colangelo, Martin Hoferichter, and Peter Stoffer, “Two-pion contribution to hadronic vacuum polarization,” *JHEP* **02**, 006 (2019), [arXiv:1810.00007 \[hep-ph\]](#); Martin Hoferichter, Bai-Long Hoid, and Bastian Kubis, “Three-pion contribution to hadronic vacuum polarization,” *JHEP* **08**, 137 (2019), [arXiv:1907.01556 \[hep-ph\]](#); M. Davier, A. Hoecker, B. Malaescu, and Z. Zhang, “A new evaluation of the hadronic vacuum polarisation contributions to the muon anomalous magnetic moment and to $\alpha(m_Z^2)$,” *Eur. Phys. J. C* **80**, 241 (2020), [Erratum: *Eur. Phys. J. C* **80**, 410 (2020)], [arXiv:1908.00921 \[hep-ph\]](#); Alexander Keshavarzi, Daisuke Nomura, and Thomas Teubner, “The $g-2$ of charged leptons, $\alpha(m_Z^2)$ and the hyperfine splitting of muonium,” *Phys. Rev. D* **101**, 014029 (2020), [arXiv:1911.00367 \[hep-ph\]](#); Alexander Kurz, Tao Liu, Peter Marquard, and Matthias Steinhauser, “Hadronic contribution to the muon anomalous magnetic moment to next-to-next-to-leading order,” *Phys. Lett. B* **734**, 144–147 (2014), [arXiv:1403.6400 \[hep-ph\]](#).
- [4] D. P. Aguillard *et al.* (Muon $g-2$), “Measurement of the Positive Muon Anomalous Magnetic Moment to 0.20 ppm,” *Phys. Rev. Lett.* **131**, 161802 (2023), [arXiv:2308.06230 \[hep-ex\]](#); G. W. Bennett *et al.* (Muon $g-2$), “Final Report of the Muon E821 Anomalous Magnetic Moment Measurement at BNL,” *Phys. Rev. D* **73**, 072003 (2006), [arXiv:hep-ex/0602035](#); B. Abi *et al.* (Muon $g-2$), “Measurement of the Positive Muon Anomalous Magnetic Moment to 0.46 ppm,” *Phys. Rev. Lett.* **126**, 141801 (2021), [arXiv:2104.03281 \[hep-ex\]](#).
- [5] Peter Athron, Csaba Balázs, Douglas H. J. Jacob, Wojciech Kotlarski, Dominik Stöckinger, and Hyejung Stöckinger-Kim, “New physics explanations of a_μ in light of the FNAL muon $g-2$ measurement,” *JHEP* **09**, 080 (2021), [arXiv:2104.03691 \[hep-ph\]](#).
- [6] H. Georgi and S. L. Glashow, “Unity of All Elementary Particle Forces,” *Phys. Rev. Lett.* **32**, 438–441 (1974).
- [7] Jogesh C. Pati and Abdus Salam, “Lepton Number as the Fourth Color,” *Phys. Rev. D* **10**, 275–289 (1974), [Erratum: *Phys. Rev. D* **11**, 703–703 (1975)].
- [8] Innes Bigaran and Raymond R. Volkas, “Getting chirality right: Single scalar leptoquark solutions to the $(g-2)_{e,\mu}$ puzzle,” *Phys. Rev. D* **102**, 075037 (2020), [arXiv:2002.12544 \[hep-ph\]](#); Ilja Doršner, Svetlana Fajfer, and Shaikh Saad, “ $\mu \rightarrow e\gamma$ selecting scalar leptoquark solutions for the $(g-2)_{e,\mu}$ puzzles,” *Phys. Rev. D* **102**, 075007 (2020), [arXiv:2006.11624 \[hep-ph\]](#); Innes Bigaran and Raymond R. Volkas, “Reflecting on chirality: CP-violating extensions of the single scalar-leptoquark solutions for the $(g-2)_{e,\mu}$ puzzles and their implications for lepton EDMs,” *Phys. Rev. D* **105**, 015002 (2022), [arXiv:2110.03707 \[hep-ph\]](#).
- [9] Farinaldo S. Queiroz and William Shepherd, “New Physics Contributions to the Muon Anomalous Magnetic Moment: A Numerical Code,” *Phys. Rev. D* **89**, 095024 (2014), [arXiv:1403.2309 \[hep-ph\]](#); Andreas Crivellin, Martin Hoferichter, and Philipp Schmidt-Wellenburg, “Combined explanations of $(g-2)_{\mu,e}$ and implications for a large muon EDM,” *Phys. Rev. D* **98**, 113002 (2018), [arXiv:1807.11484 \[hep-ph\]](#); Kamila Kowalska, Enrico Maria Sessolo, and Yasuhiro Yamamoto, “Constraints on charmphilic solutions to the muon $g-2$ with leptoquarks,” *Phys. Rev. D* **99**, 055007 (2019), [arXiv:1812.06851 \[hep-ph\]](#); Alakabha Datta, Jonathan L. Feng, Saeed Kamali, and Jacky Kumar, “Resolving the $(g-2)_\mu$ and B Anomalies with Lep-

- toquarks and a Dark Higgs Boson,” *Phys. Rev. D* **101**, 035010 (2020), [arXiv:1908.08625 \[hep-ph\]](#); Andreas Crivellin and Martin Hoferichter, “Consequences of chirally enhanced explanations of $(g-2)_\mu$ for $h \rightarrow \mu\mu$ and $Z \rightarrow \mu\mu$,” *JHEP* **07**, 135 (2021), [Erratum: *JHEP* **10**, 030 (2022)], [arXiv:2104.03202 \[hep-ph\]](#); Mingxuan Du, Jinhan Liang, Zuwei Liu, and Van Que Tran, “A vector leptoquark interpretation of the muon $g-2$ and B anomalies,” (2021), [arXiv:2104.05685 \[hep-ph\]](#); Kayoung Ban, Yongsoo Jho, Youngjoon Kwon, Seong Chan Park, Seokhee Park, and Po-Yan Tseng, “A comprehensive study of the vector leptoquark with $U(1)_{B_3-L_2}$ on the B -meson and muon $(g-2)$ anomalies,” *PTEP* **2023**, 013B01 (2023), [arXiv:2104.06656 \[hep-ph\]](#); Bingrong Yu and Shun Zhou, “General remarks on the one-loop contributions to the muon anomalous magnetic moment,” *Nucl. Phys. B* **975**, 115674 (2022), [arXiv:2106.11291 \[hep-ph\]](#); Kingman Cheung, Wai-Yee Keung, and Po-Yan Tseng, “Isodoublet vector leptoquark solution to the muon $g-2$, R_{K,K^*} , R_{D,D^*} , and W -mass anomalies,” *Phys. Rev. D* **106**, 015029 (2022), [arXiv:2204.05942 \[hep-ph\]](#).
- [10] Wolfgang Altmannshofer, Stefania Gori, Hiren H. Patel, Stefano Profumo, and Douglas Tuckler, “Electric dipole moments in a leptoquark scenario for the B -physics anomalies,” *JHEP* **05**, 069 (2020), [arXiv:2002.01400 \[hep-ph\]](#).
- [11] Luca Di Luzio, Admir Greljo, and Marco Nardecchia, “Gauge leptoquark as the origin of B -physics anomalies,” *Phys. Rev. D* **96**, 115011 (2017), [arXiv:1708.08450 \[hep-ph\]](#); Luca Di Luzio, Javier Fuentes-Martin, Admir Greljo, Marco Nardecchia, and Sophie Renner, “Maximal Flavour Violation: a Cabibbo mechanism for leptoquarks,” *JHEP* **11**, 081 (2018), [arXiv:1808.00942 \[hep-ph\]](#).
- [12] Javier Fuentes-Martín, Gino Isidori, Matthias König, and Nudžeim Selimović, “Vector Leptoquarks Beyond Tree Level,” *Phys. Rev. D* **101**, 035024 (2020), [arXiv:1910.13474 \[hep-ph\]](#); “Vector leptoquarks beyond tree level. II. $\mathcal{O}(\alpha_s)$ corrections and radial modes,” *Phys. Rev. D* **102**, 035021 (2020), [arXiv:2006.16250 \[hep-ph\]](#); “Vector Leptoquarks Beyond Tree Level III: Vector-like Fermions and Flavor-Changing Transitions,” *Phys. Rev. D* **102**, 115015 (2020), [arXiv:2009.11296 \[hep-ph\]](#); Ulrich Haisch, Luc Schnell, and Stefan Schulte, “Drell-Yan production in third-generation gauge vector leptoquark models at NLO+PS in QCD,” *JHEP* **02**, 070 (2023), [arXiv:2209.12780 \[hep-ph\]](#).
- [13] Nima Assad, Bartosz Fornal, and Benjamin Grinstein, “Baryon Number and Lepton Universality Violation in Leptoquark and Diquark Models,” *Phys. Lett. B* **777**, 324–331 (2018), [arXiv:1708.06350 \[hep-ph\]](#).
- [14] Lorenzo Calibbi, Andreas Crivellin, and Tianjun Li, “Model of vector leptoquarks in view of the B -physics anomalies,” *Phys. Rev. D* **98**, 115002 (2018), [arXiv:1709.00692 \[hep-ph\]](#); Marzia Bordone, Claudia Cornella, Javier Fuentes-Martin, and Gino Isidori, “A three-site gauge model for flavor hierarchies and flavor anomalies,” *Phys. Lett. B* **779**, 317–323 (2018), [arXiv:1712.01368 \[hep-ph\]](#); Riccardo Barbieri and Andrea Tesi, “ B -decay anomalies in Pati-Salam $SU(4)$,” *Eur. Phys. J. C* **78**, 193 (2018), [arXiv:1712.06844 \[hep-ph\]](#); Monika Blanke and Andreas Crivellin, “ B Meson Anomalies in a Pati-Salam Model within the Randall-Sundrum Background,” *Phys. Rev. Lett.* **121**, 011801 (2018), [arXiv:1801.07256 \[hep-ph\]](#); Admir Greljo and Ben A. Stefanek, “Third family quark-lepton unification at the TeV scale,” *Phys. Lett. B* **782**, 131–138 (2018), [arXiv:1802.04274 \[hep-ph\]](#); Marzia Bordone, Claudia Cornella, Javier Fuentes-Martín, and Gino Isidori, “Low-energy signatures of the PS^3 model: from B -physics anomalies to LFV,” *JHEP* **10**, 148 (2018), [arXiv:1805.09328 \[hep-ph\]](#); Julian Heeck and Daniele Teresi, “Pati-Salam explanations of the B -meson anomalies,” *JHEP* **12**, 103 (2018), [arXiv:1808.07492 \[hep-ph\]](#); Bartosz Fornal, Sri Aditya Gadam, and Benjamin Grinstein, “Left-Right $SU(4)$ Vector Leptoquark Model for Flavor Anomalies,” *Phys. Rev. D* **99**, 055025 (2019), [arXiv:1812.01603 \[hep-ph\]](#); Shyam Balaji, Robert Foot, and Michael A. Schmidt, “Chiral $SU(4)$ explanation of the $b \rightarrow s$ anomalies,” *Phys. Rev. D* **99**, 015029 (2019), [arXiv:1809.07562 \[hep-ph\]](#); Shyam Balaji and Michael A. Schmidt, “Unified $SU(4)$ theory for the $R_{D^{(*)}}$ and $R_{K^{(*)}}$ anomalies,” *Phys. Rev. D* **101**, 015026 (2020), [arXiv:1911.08873 \[hep-ph\]](#); Syuhei Iguro, Junichiro Kawamura, Shohei Okawa, and Yuji Omura, “TeV-scale vector leptoquark from Pati-Salam unification with vectorlike families,” *Phys. Rev. D* **104**, 075008 (2021), [arXiv:2103.11889 \[hep-ph\]](#); Hedvika Gedeonová and Matěj Hudec, “All possible first signals of gauge leptoquark in quark-lepton unification and beyond,” *Phys. Rev. D* **107**, 095029 (2023), [arXiv:2210.00347 \[hep-ph\]](#); Mario Fernández Navarro and Stephen F. King, “ B -anomalies in a twin Pati-Salam theory of flavour including the 2022 LHCb $R_{K^{(*)}}$ analysis,” *JHEP* **02**, 188 (2023), [arXiv:2209.00276 \[hep-ph\]](#).
- [15] Michael J. Baker, Javier Fuentes-Martín, Gino Isidori, and Matthias König, “High- p_T signatures in vector-leptoquark models,” *Eur. Phys. J. C* **79**, 334 (2019), [arXiv:1901.10480 \[hep-ph\]](#).
- [16] Leandro Da Rold and Federico Lamagna, “A vector leptoquark for the B -physics anomalies from a composite GUT,” *JHEP* **12**, 112 (2019), [arXiv:1906.11666 \[hep-ph\]](#).
- [17] Rodrigo Alonso, Benjamín Grinstein, and Jorge Martín Camalich, “Lepton universality violation and lepton flavor conservation in B -meson decays,” *JHEP* **10**, 184 (2015), [arXiv:1505.05164 \[hep-ph\]](#); Admir Greljo, Gino Isidori, and David Marzocca, “On the breaking of Lepton Flavor Universality in B decays,” *JHEP* **07**, 142 (2015), [arXiv:1506.01705 \[hep-ph\]](#); Svjetlana Fajfer and Nejc Košnik, “Vector leptoquark resolution of R_K and $R_{D^{(*)}}$ puzzles,” *Phys. Lett. B* **755**, 270–274 (2016), [arXiv:1511.06024 \[hep-ph\]](#); Riccardo Barbieri, Gino Isidori, Andrea Pattori, and Fabrizio Senia, “Anomalies in B -decays and $U(2)$ flavour symmetry,” *Eur. Phys. J. C* **76**, 67 (2016), [arXiv:1512.01560 \[hep-ph\]](#); Damir Bečirević, Nejc Košnik, Olcyr Sumensari, and Renata Zukanovich Funchal, “Palatable Leptoquark Scenarios for Lepton Flavor Violation in Exclusive $b \rightarrow s \ell_1 \ell_2$ modes,” *JHEP* **11**, 035 (2016), [arXiv:1608.07583 \[hep-ph\]](#); Suchismita Sahoo, Rukmani Mohanta, and Anjan K. Giri, “Explaining the R_K and $R_{D^{(*)}}$ anomalies with vector leptoquarks,” *Phys. Rev. D* **95**, 035027 (2017), [arXiv:1609.04367 \[hep-ph\]](#); Darius A. Faroughy, Admir Greljo, and Jernej F. Kamenik, “Confronting lepton flavor universality violation in B decays with high- p_T tau lepton searches at LHC,” *Phys. Lett. B* **764**, 126–134 (2017), [arXiv:1609.07138 \[hep-ph\]](#); Bhuvanajyoti Bhattacharya, Alakabha Datta, Jean-Pascal Guévin, David London, and Ryoutaro Watanabe, “Simultaneous Explanation of the R_K and $R_{D^{(*)}}$ Puzzles: a Model Analysis,” *JHEP* **01**, 015 (2017), [arXiv:1609.09078 \[hep-ph\]](#); Murugeswaran Duraisamy, Suchismita Sahoo, and Rukmani Mohanta, “Rare semileptonic $B \rightarrow K(\pi) l_i^- l_j^+$ decay in a vector leptoquark model,” *Phys. Rev. D* **95**, 035022 (2017), [arXiv:1610.00902 \[hep-ph\]](#); Jacky Kumar, David London, and Ryoutaro Watanabe, “Combined Explanations of the $b \rightarrow s \mu^+ \mu^-$ and $b \rightarrow c \tau^- \bar{\nu}$ Anomalies: a General Model Analysis,” *Phys. Rev. D* **99**, 015007

- (2019), [arXiv:1806.07403 \[hep-ph\]](#); Andreas Crivellin, Christoph Greub, Dario Müller, and Francesco Saturnino, “Importance of Loop Effects in Explaining the Accumulated Evidence for New Physics in B Decays with a Vector Leptoquark,” *Phys. Rev. Lett.* **122**, 011805 (2019), [arXiv:1807.02068 \[hep-ph\]](#); A. Angelescu, Damir Bečirević, D. A. Faroughy, and O. Sumensari, “Closing the window on single leptoquark solutions to the B -physics anomalies,” *JHEP* **10**, 183 (2018), [arXiv:1808.08179 \[hep-ph\]](#); Bhavesh Chauhan and Subhendra Mohanty, “Leptoquark solution for both the flavor and ANITA anomalies,” *Phys. Rev. D* **99**, 095018 (2019), [arXiv:1812.00919 \[hep-ph\]](#); C. Hati, J. Kriewald, J. Orloff, and A.M. Teixeira, “A nonunitary interpretation for a single vector leptoquark combined explanation to the B -decay anomalies,” *JHEP* **12**, 006 (2019), [arXiv:1907.05511 \[hep-ph\]](#); Claudia Cornella, Javier Fuentes-Martin, and Gino Isidori, “Revisiting the vector leptoquark explanation of the B -physics anomalies,” *JHEP* **07**, 168 (2019), [arXiv:1903.11517 \[hep-ph\]](#); Kingman Cheung, Zhuo-Ran Huang, Hua-Dong Li, Cai-Dian Lü, Ying-Nan Mao, and Ru-Ying Tang, “Revisit to the $b \rightarrow c\tau\nu$ transition: In and beyond the SM,” *Nucl. Phys. B* **965**, 115354 (2021), [arXiv:2002.07272 \[hep-ph\]](#); P. S. Bhupal Dev, Rukmani Mohanta, Sudhanwa Patra, and Suchismita Sahoo, “Unified explanation of flavor anomalies, radiative neutrino masses, and ANITA anomalous events in a vector leptoquark model,” *Phys. Rev. D* **102**, 095012 (2020), [arXiv:2004.09464 \[hep-ph\]](#); C. Hati, J. Kriewald, J. Orloff, and A. M. Teixeira, “The fate of V_1 vector leptoquarks: the impact of future flavour data,” *Eur. Phys. J. C* **81**, 1066 (2021), [arXiv:2012.05883 \[hep-ph\]](#); Andrei Angelescu, Damir Bečirević, Darius A. Faroughy, Florentin Jaffredo, and Olcyr Sumensari, “Single leptoquark solutions to the B -physics anomalies,” *Phys. Rev. D* **104**, 055017 (2021), [arXiv:2103.12504 \[hep-ph\]](#); Claudia Cornella, Darius A. Faroughy, Javier Fuentes-Martin, Gino Isidori, and Matthias Neubert, “Reading the footprints of the B -meson flavor anomalies,” *JHEP* **08**, 050 (2021), [arXiv:2103.16558 \[hep-ph\]](#); Stephen F. King, “Twin Pati-Salam theory of flavour with a TeV scale vector leptoquark,” *JHEP* **11**, 161 (2021), [arXiv:2106.03876 \[hep-ph\]](#); Geneviève Bélanger, Jacky Kumar, David London, and Alexander Pukhov, “The B anomalies, the U_1 leptoquark and dark matter,” *JHEP* **01**, 041 (2023), [arXiv:2206.11305 \[hep-ph\]](#); Riccardo Barbieri, Claudia Cornella, and Gino Isidori, “Simplified models of vector $SU(4)$ leptoquarks at the TeV,” *Eur. Phys. J. C* **82**, 1161 (2022), [arXiv:2207.14248 \[hep-ph\]](#); Cristian H. García-Duque, J. M. Cabarcas, J. H. Muñoz, Néstor Quintero, and Eduardo Rojas, “Singlet vector leptoquark model facing recent LHCb and BABAR measurements,” *Nucl. Phys. B* **988**, 116115 (2023), [arXiv:2209.04753 \[hep-ph\]](#).
- [18] Dario Buttazzo, Admir Greljo, Gino Isidori, and David Marzocca, “ B -physics anomalies: a guide to combined explanations,” *JHEP* **11**, 044 (2017), [arXiv:1706.07808 \[hep-ph\]](#).
- [19] Jason Aebischer, Gino Isidori, Marko Pesut, Ben A. Stefanek, and Felix Wilsch, “Confronting the vector leptoquark hypothesis with new low- and high-energy data,” *Eur. Phys. J. C* **83**, 153 (2023), [arXiv:2210.13422 \[hep-ph\]](#).
- [20] Tanumoy Mandal, Subhadip Mitra, and Swapnil Raz, “ $R_{D^{(*)}}$ motivated S_1 leptoquark scenarios: Impact of interference on the exclusion limits from LHC data,” *Phys. Rev. D* **99**, 055028 (2019), [arXiv:1811.03561 \[hep-ph\]](#); Ufuk Aydemir, Tanumoy Mandal, and Subhadip Mitra, “Addressing the $R_{D^{(*)}}$ anomalies with an S_1 leptoquark from $SO(10)$ grand unification,” *Phys. Rev. D* **101**, 015011 (2020), [arXiv:1902.08108 \[hep-ph\]](#); Arvind Bhaskar, Anirudhan A. Madathil, Tanumoy Mandal, and Subhadip Mitra, “Combined explanation of W -mass, muon $g-2$, R_K^* and R_D^* anomalies in a singlet-triplet scalar leptoquark model,” *Phys. Rev. D* **106**, 115009 (2022), [arXiv:2204.09031 \[hep-ph\]](#); Ufuk Aydemir, Tanumoy Mandal, Subhadip Mitra, and Shoaib Munir, “An economical model for B -flavour and a_μ anomalies from $SO(10)$ grand unification,” (2022), [arXiv:2209.04705 \[hep-ph\]](#).
- [21] Arvind Bhaskar, Diganta Das, Tanumoy Mandal, Subhadip Mitra, and Cyrin Neeraj, “Precise limits on the charge-2/3 U_1 vector leptoquark,” *Phys. Rev. D* **104**, 035016 (2021), [arXiv:2101.12069 \[hep-ph\]](#).
- [22] Arvind Bhaskar, Arijit Das, Tanumoy Mandal, Subhadip Mitra, and Rachit Sharma, “Fresh look at the LHC limits on scalar leptoquarks,” *Phys. Rev. D* **109**, 055018 (2024), [arXiv:2312.09855 \[hep-ph\]](#).
- [23] Tanumoy Mandal, Subhadip Mitra, and Satyajit Seth, “Single Productions of Colored Particles at the LHC: An Example with Scalar Leptoquarks,” *JHEP* **07**, 028 (2015), [arXiv:1503.04689 \[hep-ph\]](#).
- [24] Tanumoy Mandal, Subhadip Mitra, and Satyajit Seth, “Pair Production of Scalar Leptoquarks at the LHC to NLO Parton Shower Accuracy,” *Phys. Rev. D* **93**, 035018 (2016), [arXiv:1506.07369 \[hep-ph\]](#); Kushagra Chandak, Tanumoy Mandal, and Subhadip Mitra, “Hunting for scalar leptoquarks with boosted tops and light leptons,” *Phys. Rev. D* **100**, 075019 (2019), [arXiv:1907.11194 \[hep-ph\]](#); Arvind Bhaskar, Tanumoy Mandal, and Subhadip Mitra, “Boosting vector leptoquark searches with boosted tops,” *Phys. Rev. D* **101**, 115015 (2020), [arXiv:2004.01096 \[hep-ph\]](#); Arvind Bhaskar, Tanumoy Mandal, Subhadip Mitra, and Mohit Sharma, “Improving third-generation leptoquark searches with combined signals and boosted top quarks,” *Phys. Rev. D* **104**, 075037 (2021), [arXiv:2106.07605 \[hep-ph\]](#); Kingman Cheung, Thong T. Q. Nguyen, and C. J. Ouseph, “Leptoquark search at the Forward Physics Facility,” *Phys. Rev. D* **108**, 036014 (2023), [arXiv:2302.05461 \[hep-ph\]](#); A. Flórez, J. Jones-Pérez, A. Gurrola, C. Rodríguez, and J. Peñuela Parra, “On the sensitivity reach of LQ production with preferential couplings to third generation fermions at the LHC,” *Eur. Phys. J. C* **83**, 1023 (2023), [arXiv:2307.11070 \[hep-ph\]](#).
- [25] M. J. Musolf and Barry R. Holstein, “Observability of the anapole moment and neutrino charge radius,” *Phys. Rev. D* **43**, 2956–2970 (1991).
- [26] Sz. Borsanyi *et al.*, “Leading hadronic contribution to the muon magnetic moment from lattice QCD,” *Nature* **593**, 51–55 (2021), [arXiv:2002.12347 \[hep-lat\]](#).
- [27] F. V. Ignatov *et al.* (CMD-3), “Measurement of the $e^+e^- \rightarrow \pi^+\pi^-$ cross section from threshold to 1.2 GeV with the CMD-3 detector,” *Phys. Rev. D* **109**, 112002 (2024), [arXiv:2302.08834 \[hep-ex\]](#).
- [28] Richard H. Parker, Chenghui Yu, Weicheng Zhong, Brian Estey, and Holger Müller, “Measurement of the fine-structure constant as a test of the Standard Model,” *Science* **360**, 191 (2018), [arXiv:1812.04130 \[physics.atom-ph\]](#).
- [29] Léo Morel, Zhibin Yao, Pierre Cladé, and Saïda Guellati-Khélifa, “Determination of the fine-structure constant with an accuracy of 81 parts per trillion,” *Nature* **588**, 61–65 (2020).
- [30] “Observation of $\gamma\gamma \rightarrow \tau\tau$ in proton-proton collisions and limits on the anomalous electromagnetic moments of the τ lepton,” *Rep. Prog. Phys.* **87**, 107801 (2024), [arXiv:2406.03975 \[hep-ex\]](#).
- [31] J. Abdallah *et al.* (DELPHI), “Study of tau-pair production in photon-photon collisions at LEP and limits on the anoma-

- lous electromagnetic moments of the tau lepton,” *Eur. Phys. J. C* **35**, 159–170 (2004), [arXiv:hep-ex/0406010](#).
- [32] R. L. Workman *et al.* (Particle Data Group), “Review of Particle Physics,” *PTEP* **2022**, 083C01 (2022).
- [33] S. Eidelman and M. Passera, “Theory of the tau lepton anomalous magnetic moment,” *Mod. Phys. Lett. A* **22**, 159–179 (2007), [arXiv:hep-ph/0701260](#).
- [34] Uma Mahanta, “Dipole moments of τ as a sensitive probe for beyond standard model physics,” *Phys. Rev. D* **54**, 3377–3381 (1996), [arXiv:hep-ph/9604380](#).
- [35] Yasuhiro Yamaguchi and Nodoka Yamanaka, “Large long-distance contributions to the electric dipole moments of charged leptons in the standard model,” *Phys. Rev. Lett.* **125**, 241802 (2020), [arXiv:2003.08195 \[hep-ph\]](#).
- [36] Yasuhiro Yamaguchi and Nodoka Yamanaka, “Quark level and hadronic contributions to the electric dipole moment of charged leptons in the standard model,” *Phys. Rev. D* **103**, 013001 (2021), [arXiv:2006.00281 \[hep-ph\]](#).
- [37] V. Andreev *et al.* (ACME), “Improved limit on the electric dipole moment of the electron,” *Nature* **562**, 355–360 (2018).
- [38] G. W. Bennett *et al.* (Muon (g-2)), “An Improved Limit on the Muon Electric Dipole Moment,” *Phys. Rev. D* **80**, 052008 (2009), [arXiv:0811.1207 \[hep-ex\]](#).
- [39] K. Inami *et al.* (Belle), “Search for the electric dipole moment of the tau lepton,” *Phys. Lett. B* **551**, 16–26 (2003), [arXiv:hep-ex/0210066](#).
- [40] W. Buchmuller, R. Ruckl, and D. Wyler, “Leptoquarks in Lepton - Quark Collisions,” *Phys. Lett. B* **191**, 442–448 (1987), [Erratum: *Phys. Lett. B* 448, 320–320 (1999)].
- [41] I. Doršner, S. Fajfer, A. Greljo, J. F. Kamenik, and N. Košnik, “Physics of leptoquarks in precision experiments and at particle colliders,” *Phys. Rept.* **641**, 1–68 (2016), [arXiv:1603.04993 \[hep-ph\]](#).
- [42] Johannes Blumlein, Edward Boos, and Alexander Kryukov, “Leptoquark pair production in hadronic interactions,” *Z. Phys. C* **76**, 137–153 (1997), [arXiv:hep-ph/9610408](#).
- [43] Alexander Belyaev, Claude Leroy, Rashid Mehdiev, and Alexander Pukhov, “Leptoquark single and pair production at LHC with CalcHEP/CompHEP in the complete model,” *JHEP* **09**, 005 (2005), [arXiv:hep-ph/0502067](#).
- [44] J. Blumlein and R. Ruckl, “Production of scalar and vector leptoquarks in e^+e^- annihilation,” *Phys. Lett. B* **304**, 337–346 (1993).
- [45] Andreas Crivellin, Martin Hoferichter, and J. Michael Roney, “Toward testing the magnetic moment of the tau at one part per million,” *Phys. Rev. D* **106**, 093007 (2022), [arXiv:2111.10378 \[hep-ph\]](#).
- [46] Albert M Sirunyan *et al.* (CMS), “Constraints on models of scalar and vector leptoquarks decaying to a quark and a neutrino at $\sqrt{s} = 13$ TeV,” *Phys. Rev. D* **98**, 032005 (2018), [arXiv:1805.10228 \[hep-ex\]](#); “Search for singly and pair-produced leptoquarks coupling to third-generation fermions in proton-proton collisions at $s=13$ TeV,” *Phys. Lett. B* **819**, 136446 (2021), [arXiv:2012.04178 \[hep-ex\]](#); Georges Aad *et al.* (ATLAS), “Search for pair-produced scalar and vector leptoquarks decaying into third-generation quarks and first- or second-generation leptons in pp collisions with the ATLAS detector,” *JHEP* **2306**, 188 (2023), [arXiv:2210.04517 \[hep-ex\]](#).
- [47] Albert M Sirunyan *et al.* (CMS), “Search for resonant and nonresonant new phenomena in high-mass dilepton final states at $\sqrt{s} = 13$ TeV,” *JHEP* **07**, 208 (2021), [arXiv:2103.02708 \[hep-ex\]](#).
- [48] Tanumoy Mandal and Subhadip Mitra, “Probing Color Octet Electrons at the LHC,” *Phys. Rev. D* **87**, 095008 (2013), [arXiv:1211.6394 \[hep-ph\]](#); Tanumoy Mandal, Subhadip Mitra, and Satyajit Seth, “Probing Compositeness with the CMS $eejj$ & eej Data,” *Phys. Lett. B* **758**, 219–225 (2016), [arXiv:1602.01273 \[hep-ph\]](#); Arvind Bhaskar, Yash Chaurasia, Kuldeep Deka, Tanumoy Mandal, Subhadip Mitra, and Ananya Mukherjee, “Right-handed neutrino pair production via second-generation leptoquarks,” *Phys. Lett. B* **843**, 138039 (2023), [arXiv:2301.11889 \[hep-ph\]](#).
- [49] Arvind Bhaskar, Arijit Das, Yash Chaurasia, Atirek Kumar, Tanumoy Mandal, Subhadip Mitra, and Rachit Sharma, “TooLQit: Leptoquark Models and Limits,” In preparation (2024).
- [50] Adam Alloul, Neil D. Christensen, Céline Degrande, Claude Duhr, and Benjamin Fuks, “FeynRules 2.0 - A complete toolbox for tree-level phenomenology,” *Comput. Phys. Commun.* **185**, 2250–2300 (2014), [arXiv:1310.1921 \[hep-ph\]](#).
- [51] Céline Degrande, Claude Duhr, Benjamin Fuks, David Grellscheid, Olivier Mattelaer, and Thomas Reiter, “UFO - The Universal FeynRules Output,” *Comput. Phys. Commun.* **183**, 1201–1214 (2012), [arXiv:1108.2040 \[hep-ph\]](#).
- [52] J. Alwall, R. Frederix, S. Frixione, V. Hirschi, F. Maltoni, O. Mattelaer, H. S. Shao, T. Stelzer, P. Torrielli, and M. Zaro, “The automated computation of tree-level and next-to-leading order differential cross sections, and their matching to parton shower simulations,” *JHEP* **07**, 079 (2014), [arXiv:1405.0301 \[hep-ph\]](#).
- [53] Christian Bierlich *et al.*, “A comprehensive guide to the physics and usage of PYTHIA 8.3,” *SciPost Phys. Codeb.* **2022**, 8 (2022), [arXiv:2203.11601 \[hep-ph\]](#).
- [54] J. de Favereau, C. Delaere, P. Demin, A. Giammanco, V. Lemaître, A. Mertens, and M. Selvaggi (DELPHES 3), “DELPHES 3, A modular framework for fast simulation of a generic collider experiment,” *JHEP* **02**, 057 (2014), [arXiv:1307.6346 \[hep-ex\]](#).
- [55] C. Abel *et al.*, “Measurement of the Permanent Electric Dipole Moment of the Neutron,” *Phys. Rev. Lett.* **124**, 081803 (2020), [arXiv:2001.11966 \[hep-ex\]](#).
- [56] Jonathan Engel, Michael J. Ramsey-Musolf, and U. van Kolck, “Electric Dipole Moments of Nucleons, Nuclei, and Atoms: The Standard Model and Beyond,” *Prog. Part. Nucl. Phys.* **71**, 21–74 (2013), [arXiv:1303.2371 \[nucl-th\]](#).
- [57] Syuhei Iguro and Teppei Kitahara, “Electric dipole moments as probes of the R_D^* anomaly,” *Phys. Rev. D* **110**, 075008 (2024), [arXiv:2307.11751 \[hep-ph\]](#).
- [58] D. Androić *et al.* (Qweak), “Precision measurement of the weak charge of the proton,” *Nature* **557**, 207–211 (2018), [arXiv:1905.08283 \[nucl-ex\]](#).
- [59] Saurabh Bansal, Rodolfo M. Capdevilla, and Christopher Kolda, “Constraining the minimal flavor violating leptoquark explanation of the $R_{D^{(*)}}$ anomaly,” *Phys. Rev. D* **99**, 035047 (2019), [arXiv:1810.11588 \[hep-ph\]](#).
- [60] Hiren H. Patel, “Package-X 2.0: A Mathematica package for the analytic calculation of one-loop integrals,” *Comput. Phys. Commun.* **218**, 66–70 (2017), [arXiv:1612.00009 \[hep-ph\]](#).